

# Selective alkylation of mandelic acid to diarylacetic acids over a commercial zeolite

Sam G. Meacham<sup>a</sup> and Russell A. Taylor<sup>a\*</sup>

<sup>a</sup>Department of Chemistry, Durham University, South Road, Durham DH1 3LE, UK.

\*Email: [russell.taylor@durham.ac.uk](mailto:russell.taylor@durham.ac.uk)

## Supplementary Information

1	Experimental Procedures.....	2
1.1	Materials .....	2
1.2	Catalyst Evaluation .....	2
1.3	Sample Characterisation .....	4
1.4	Characterisation of Reaction Products from Zeolite-Catalysed Conversion of Mandelic Acid in Aromatic Solvents .....	4
1.4.1	B1. Electrophilic Aromatic Substitution Reaction Products .....	6
1.4.2	B2. Benzaldehyde.....	11
1.4.3	B3. 2,5-diphenyl-1,3-dioxolan-4-one .....	12
1.4.4	Quantification Method and an Example Product Mixture Quantification .....	14
2	Effect of Reaction Conditions on Product Distribution in Mandelic Acid Conversion using H-Beta-75 and H-USY Zeolites as Catalyst .....	17
2.1	Effect of Reaction Solvent on Selectivity with H-Y-30 Catalyst.....	17
2.2	Effect of Reaction Solvent on H-Beta-75 Catalysis.....	17
2.3	Selectivity of Commercial Zeolites H-Beta-75, H-Y-30, H-MOR-97 and H-ZSM-45 at Low and Near Iso-conversion of Mandelic Acid .....	18
3	Molecular Size and Zeolite Pore Considerations .....	19
4	Zeolite Catalyst Properties.....	20
4.1	Comparison of HY series .....	22
4.2	Estimate of occluded organic matter in H-Y-30 post reaction.....	22
4.3	A comment on catalyst lifetime .....	23

# 1 Experimental Procedures

## 1.1 Materials

D,L-Mandelic acid (99+%, Acros Organics), acetonitrile (HPLC grade), benzaldehyde (Alfa Aesar, 99+%), cyclohexane (99.5%, Thermo Scientific), toluene (AR grade), o-xylene (99%), p-xylene (99%), m-xylene (99%) and mixed xylenes (AR grade) were purchased from Fisher Scientific. Chlorobenzene and para-toluenesulfonic acid monohydrate were purchased from Sigma Aldrich. All chemicals were used as received without any further purification.

Zeolite Y (CBV series) materials were purchased from Alfa Aesar or supplied by Johnson Matthey. ZSM5, Beta, L and Mordenite zeolites were supplied by Clariant. Further details of catalyst properties are given in Section S4 below. All zeolites were used as commercially supplied, without a pre-drying step or a calcination step.

The shorthand naming convention used for the commercial zeolites within this work follows the following: X-YYY-ZZ, where YYY is the zeolite framework, X is the stated counter-cation and ZZ is the Si/Al ratio, all as reported by the zeolite manufacturer.

## 1.2 Catalyst Evaluation

Reactions were carried out without the use of inert atmosphere techniques. For overnight catalyst screening tests, a round bottom flask (100 ml) was charged with mandelic acid (0.5 g), 3 mol% H<sup>+</sup> (pTSA) or 3 mol% Al (zeolites), solvent (50 ml) and a stirrer bar. For time-dependent conversion plots, a round bottom flask (50 ml) was charged with mandelic acid (0.2 g), 3 mol% H<sup>+</sup> (pTSA) or 3 mol% Al (zeolites), solvent (20 ml) and a stirrer bar was used (catalyst masses are given in Table S6). The flask was connected to a homemade phase separator with a water condenser above (Figure S1). The flask was contacted with a pre-heated hotplate set 20 °C above the solvent boiling point and stirred at 500 rpm. This was taken as time = 0.

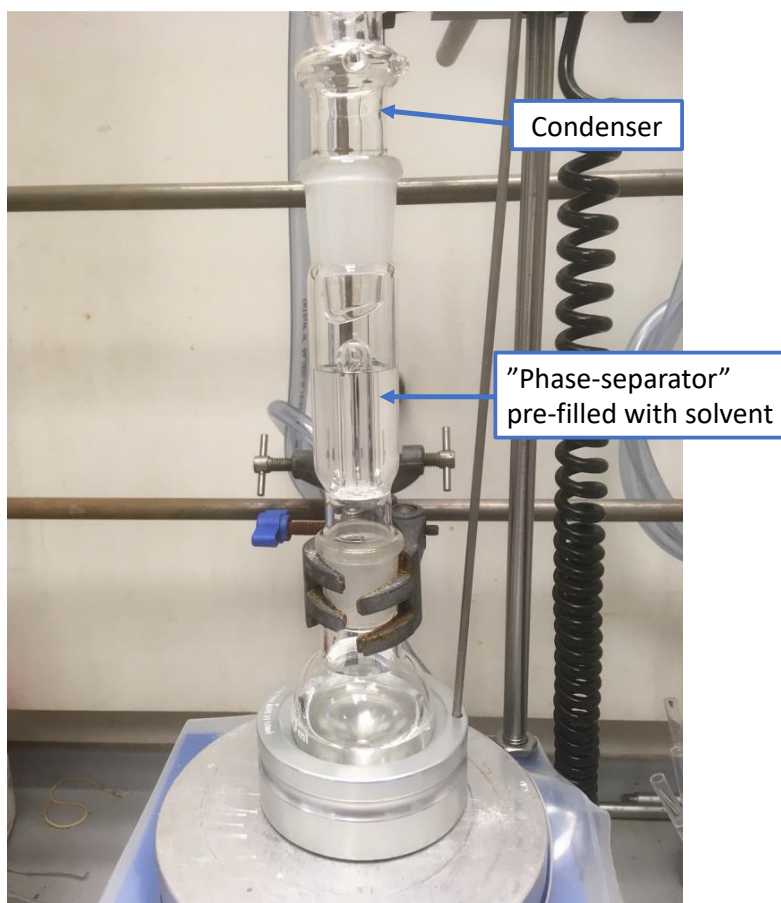


Figure S1 Reaction setup used for arylation of mandelic acid. A phase separator is used to between the flask and condenser to remove water produced during the reaction. The phase separator is pre-filled with reaction solvent to avoid a reduction in the reaction volume upon reflux.

To analyse the product distribution, the reaction mixture was allowed to cool to room temperature (approximately 10 mins) and an equal volume of acetonitrile was added to dissolve any insoluble species. The reaction mixture was then filtered by vacuum filtration (Buchner flask and filter paper) to remove the zeolite and a small sample (ca. 1 ml) of the filtrate was taken forward for analysis. Solvent was removed in vacuo and the crude sample dissolved in  $\text{CDCl}_3$  for analysis by NMR spectroscopy, to calculate the composition of products.

An additional sample was also made by diluting a couple of drops of the filtrate with 1 ml  $\text{CDCl}_3$ . This sample was used to check for the presence of volatile benzaldehyde that would otherwise be removed by rotary evaporation. When benzaldehyde was present, this sample could be used to account for this in the final quantification.

Where necessary, to confirm and isolate the presence of the cyclic products (dioxolanone and mandelide), an aqueous organic wash was performed on the crude filtrate with saturated sodium bicarbonate solution (3 x 50ml), drying the organic layer over  $\text{MgSO}_4$  followed by vacuum filtration. In the case of H-Beta-catalysed reactions, this yielded a crude mix of mandelide and dioxolanone from the organic layer, as shown in Figure S12, and was used to help identify the dioxolanone product.

For the conversion-time plots, individual reactions of different durations were carried out rather than sampling a single reaction over time. This was done to avoid issues associated with the poor solubility of some of the products at room temperature which would have adversely affected the selectivity calculations should products precipitate during sampling.

### 1.3 Sample Characterisation

Solution-state  $^1\text{H}$  and  $^{13}\text{C}$  NMR spectra were recorded on a Bruker Avance-400 spectrometer. Chemical shifts are reported in ppm using the residual solvent signal as an internal reference. All NMR spectra were manipulated using MestReNova software.

Elemental (CHN) microanalyses were obtained on an Exeter Analytical Inc. E-440 elemental analyser.

Samples for electron ionisation (EI) tandem liquid chromatography mass spectra (LC-MS) were prepared by dissolution in acetonitrile at  $\sim 1\text{mg mL}^{-1}$  and submitted via mass spectrometry service. Samples were separated on an Acquity UPLC BEH C18 column (1.7  $\mu\text{m}$ , 2.1mm x 50mm) using acetonitrile/water gradient. Mass spectra were recorded on Waters triple quadrupole mass spectrometer, using electrospray ionisation.

pXRD diffractograms were collected on a Bruker D8 avance X-ray diffractometer using a step of  $0.02^\circ$  over a range of  $2\theta = 5\text{--}70^\circ$ . A knife edge was utilised for low angle scattering. Samples were mounted onto glass or silicon slide holders and rotated during data acquisition.

Energy dispersive X-ray fluorescence (ED-XRF) analyses were performed using a Panalytical Epsilon 1 ED-XRF. The samples (approx. 0.2–1 g) were provided as homogenized powders and were pressed into discs within a sample cup containing a polypropylene film. The pressed powders were run on a Panalytical Epsilon 1 ED-XRF with a 50 kV silver anode tube. The total analysis time for each sample was around 20 minutes. The samples were analysed using the Malvern Panalytical's proprietary 'Omnian' calibration which had additional zeolite derived standards added to it to improve accuracy for specific elements, such as Si and Al. Corrections were made for the variable weight of each sample.

### 1.4 Characterisation of Reaction Products from Zeolite-Catalysed Conversion of Mandelic Acid in Aromatic Solvents

The chemical shift of the methine proton mandelic acid was experimentally determined to be 5.25 ppm (400 MHz,  $\text{CDCl}_3$ ). Chemical shifts of other compounds are assigned in Table S22. The linear dimer of mandelic acid and the isomers of mandelide were assigned based on literature reference data.<sup>1-3</sup> Other products have been identified by independent synthesis and characterisation against literature data (see Sections 1.4.1 – 1.4.3 below) The structures of all products are shown in Figure S2 and the protons used for quantification of the product compositions by  $^1\text{H}$  NMR spectroscopy are highlighted in red.

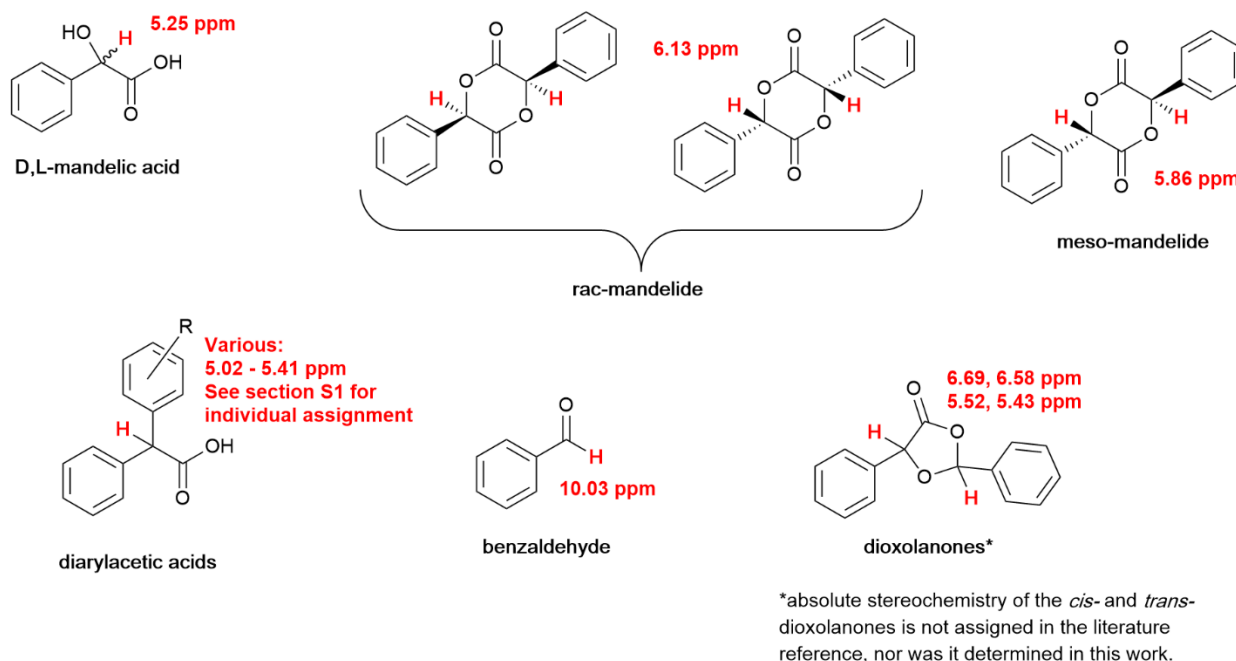


Figure S2 Structures of the products detailed in the catalyst testing reactions. Highlighted in red are the protons used for quantification of the product compositions by  $^1\text{H}$  NMR spectroscopy,  $\text{CDCl}_3$  (see Table S2 for further details).

Three compounds have been identified to consistently be present in the  $^1\text{H}$  NMR spectra of products from zeolite-catalysed reactions of mandelic acid when using H-Beta zeolite. The first of these products (B1, Figure S3) was also produced selectively by zeolite H-Y-30. A combination of NMR spectroscopy and LC-MS was used to identify these compounds. B1 was identified as the product of an electrophilic aromatic substitution (Friedel-Crafts) reaction between mandelic acid and the aromatic solvent molecules. The second, B2, has been identified as benzaldehyde and produced by H-Beta zeolites as a minor product. The third compound has been identified as 2,5-diphenyl-1,3-dioxolan-4-one (B3), the product of reaction of mandelic acid with benzaldehyde.

Ar = aromatic solvent

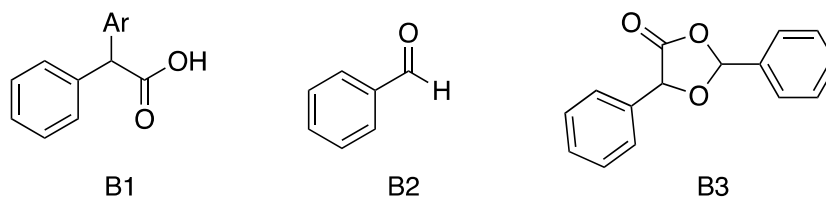


Figure S3 Significant products identified in zeolite-catalysed conversion of mandelic acid when heated to reflux in aromatic solvents with azeotropic water removal.

### 1.4.1 B1. Electrophilic Aromatic Substitution Reaction Products

Zeolite H-Y-30 was found to catalyse the electrophilic aromatic substitution reaction between mandelic acid and a range of aromatic solvents in high selectivity, and so was used to prepare reference compounds for further NMR analysis. Reaction of mandelic acid in p-xylene catalysed by H-Y-30 gave product B1 in >95% selectivity in an overnight reaction. Examples of the spectroscopic analysis obtained for the reactions of mandelic acid with p-xylene, toluene and mesitylene are shown in Figure S4 to Figure S8.

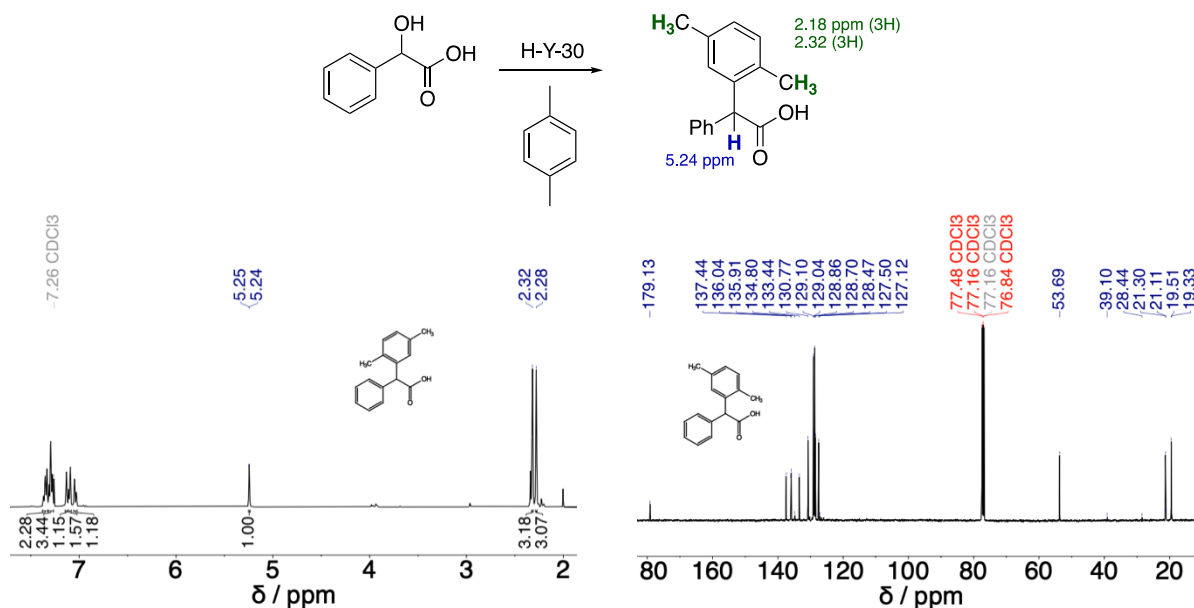


Figure S4 Reaction of mandelic acid in p-xylene. When H-Y-30 is used as catalyst, the major product observed (B1) is from an electrophilic aromatic substitution reaction. Reaction conditions: 0.2 g mandelic acid, 20 ml p-xylene, reflux with Dean Stark trap, oil bath T = 175 °C (T<sub>b</sub> + 35 °C), stirring rate = 500 rpm, time = 3 hours. <sup>1</sup>H and <sup>13</sup>C NMR spectra (400 MHz, CDCl<sub>3</sub>) showing isolated product.

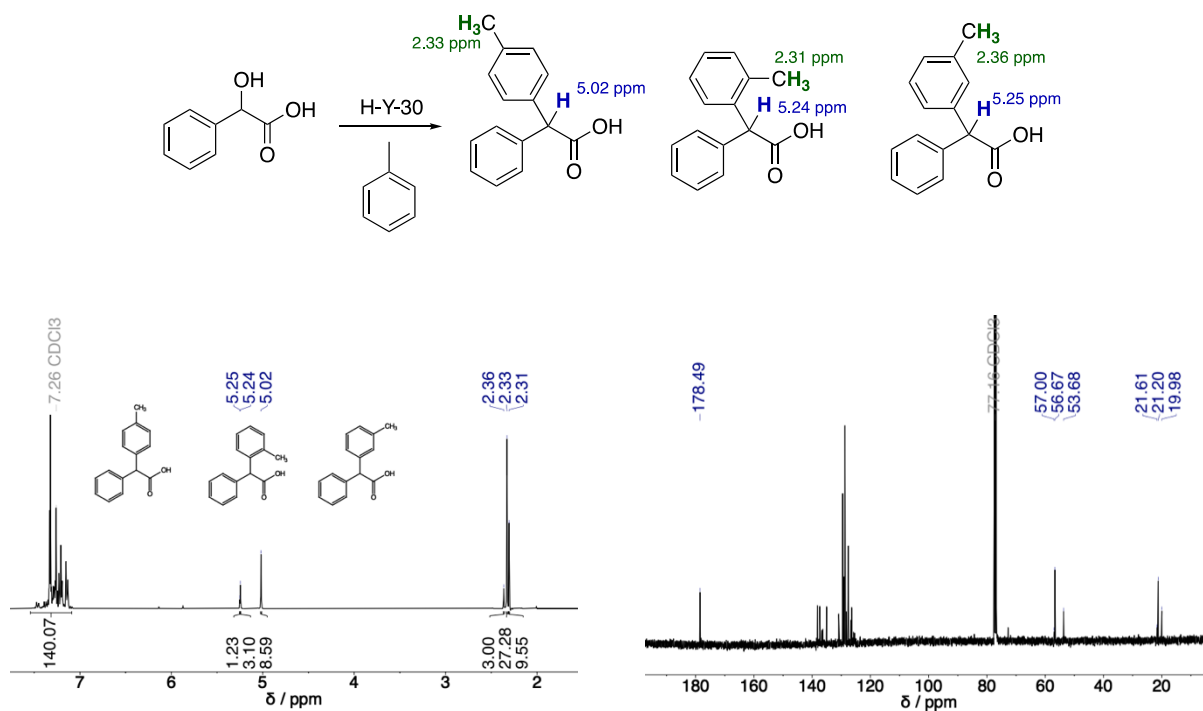


Figure S5 Reaction of mandelic acid in toluene. When H-Y-30 is used as catalyst, the major product observed (B1) is from an electrophilic aromatic substitution reaction. Ortho, para and meta isomers are formed. Reaction conditions: 0.2 g mandelic acid, 20 ml toluene, reflux with Dean Stark trap, oil bath  $T = 145^\circ\text{C}$  ( $T_b + 35^\circ\text{C}$ ), stirring rate = 500 rpm, time = 20 hours.  $^1\text{H}$  and  $^{13}\text{C}$  NMR spectra (400 MHz,  $\text{CDCl}_3$ ) show a mix of the three isomeric products.

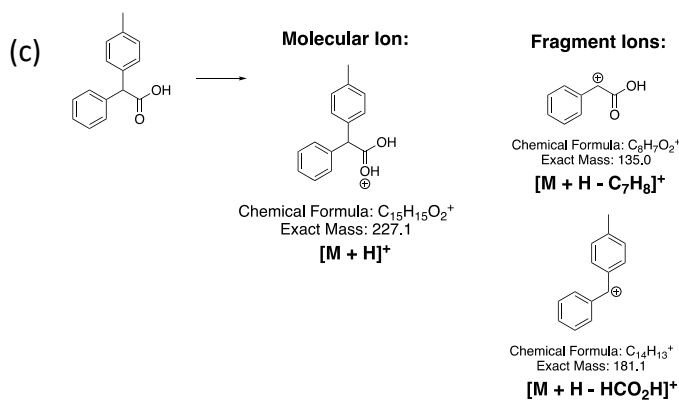
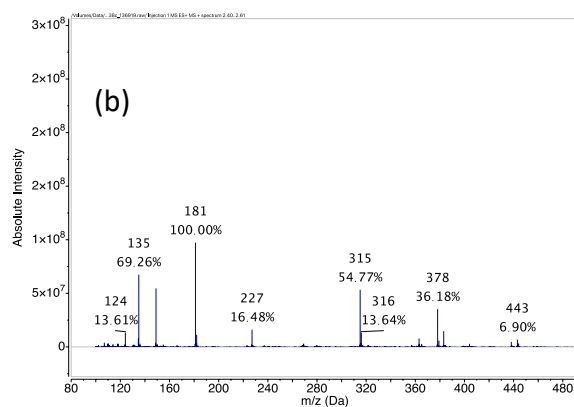
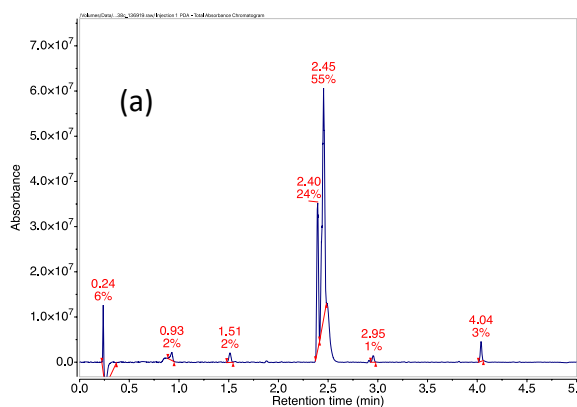


Figure S6 LC-MS analysis: (a) UV-absorbance chromatogram, (b) ESI-MS positive ion spectrum ( $R_T = 2.4\text{-}2.6$  min) for the aromatic substitution product of mandelic acid and toluene, catalysed by zeolite H-Y-30, (c) assignment of mass peaks at  $m/z$  227 Da (16%), 181 Da (100%) and 135 Da (69%).



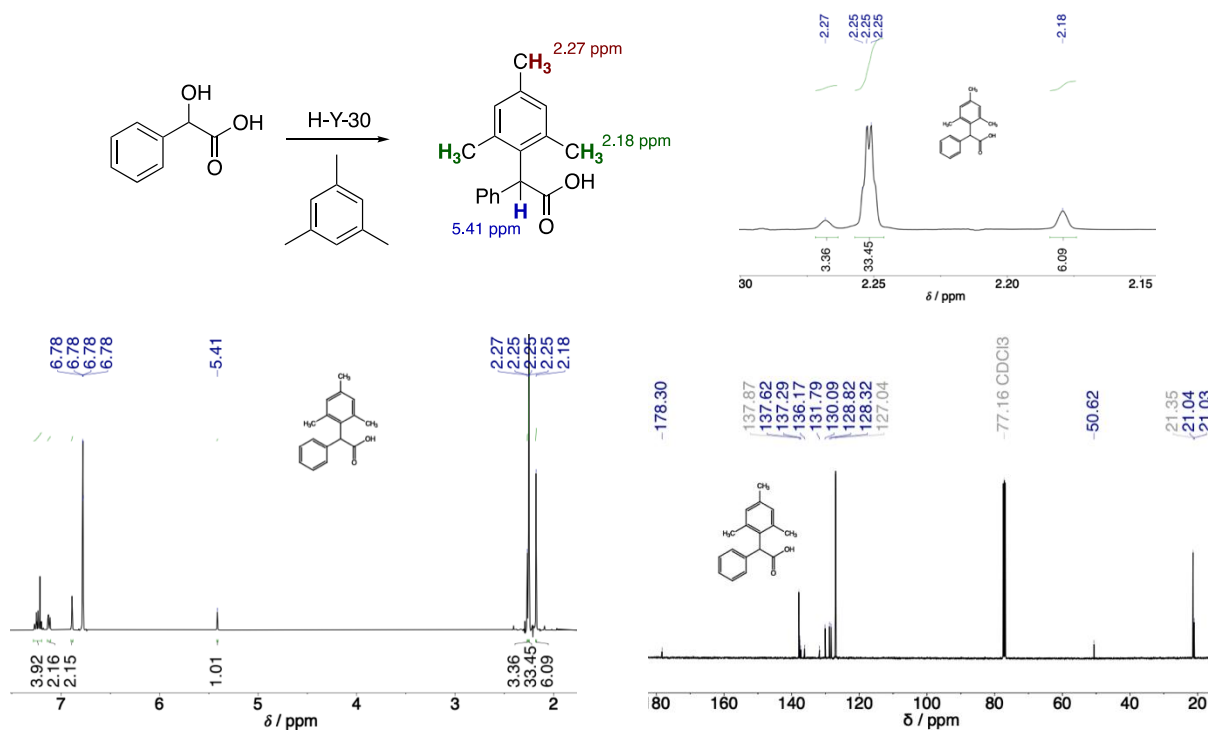


Figure S7 Reaction of mandelic acid in mesitylene. When H-Y-30 is used as catalyst, the major product observed (B1) is from an electrophilic aromatic substitution reaction. Reaction conditions: 0.2 g mandelic acid, 20 ml mesitylene, reflux with Dean Stark trap, oil bath T = 180°C (T<sub>b</sub> + 15 °C), stirring rate = 500 rpm. <sup>1</sup>H and <sup>13</sup>C NMR spectra (400 MHz, CDCl<sub>3</sub>) show isolated product. Due to the high boiling point of this solvent, some residual reaction solvent is present in the spectra (6.78 ppm, 3H and 2.25 ppm, 9H).

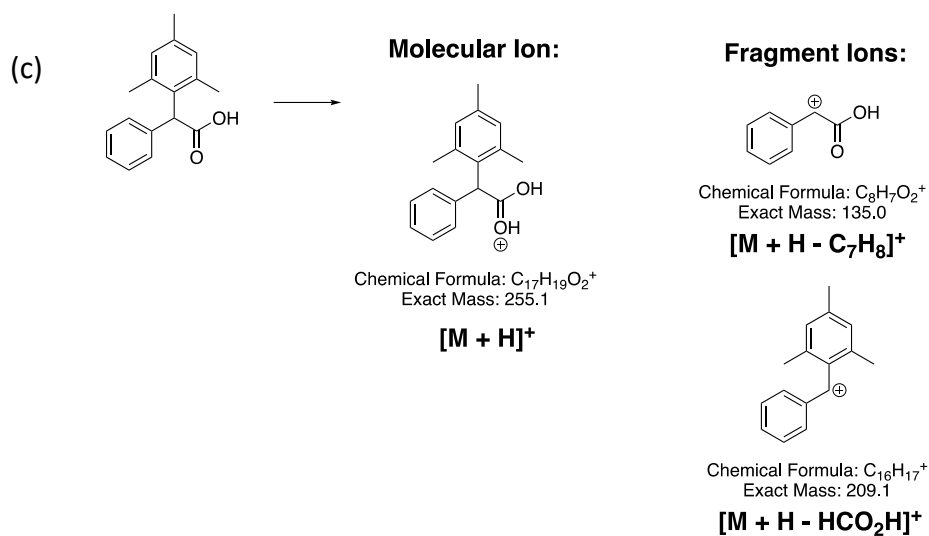
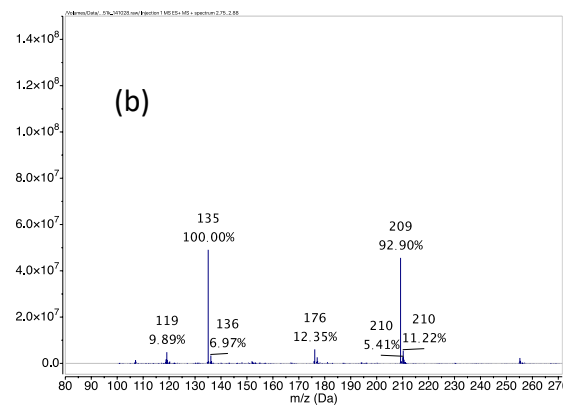
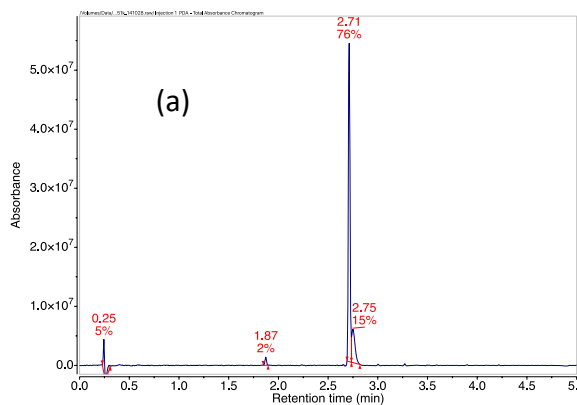


Figure S8 LC-MS analysis: (a) UV-absorbance chromatogram, (b) ESI-MS positive ion spectrum (RT = 2.75-2.88 min) for electrophilic aromatic substitution product of mandelic acid and mesitylene, catalysed by zeolite H-Y-30. (c) assignment of mass peaks at  $m/z$  255 Da (low abundance), 209 Da (93%) and 135 Da (100%).

## 1.4.2 B2. Benzaldehyde

The aldehyde proton of benzaldehyde resonates at around 10 ppm, as well as a peak at around 8 ppm for the 2H environment of aromatic protons adjacent to the aldehyde group, giving this a very clear set of peaks in  $^1\text{H}$  NMR spectra. Comparison of the  $^1\text{H}$  NMR spectrum of pure benzaldehyde with that of a crude product mixture from a zeolite catalysed reaction is shown in Figure S9, indicating the formation of benzaldehyde. This can occur via two possible pathways, by loss of  $\text{CO}$  and  $\text{H}_2\text{O}$  (decarbonylation) or  $\text{CO}_2$  and  $\text{H}_2$  (decarboxylation). Literature reports suggest decomposition of mandelic acid at high temperatures leads to benzaldehyde formation via a decarbonylative pathway, and in some cases is proposed to occur via an alpha-lactone intermediate due to loss of the alpha hydroxy group.<sup>1</sup> This could feasibly occur through a Brønsted acid-catalysed process, from protonation of the alpha-OH and subsequent attack by the carboxylic acid group to form the alpha-lactone (Figure S10).<sup>4</sup>

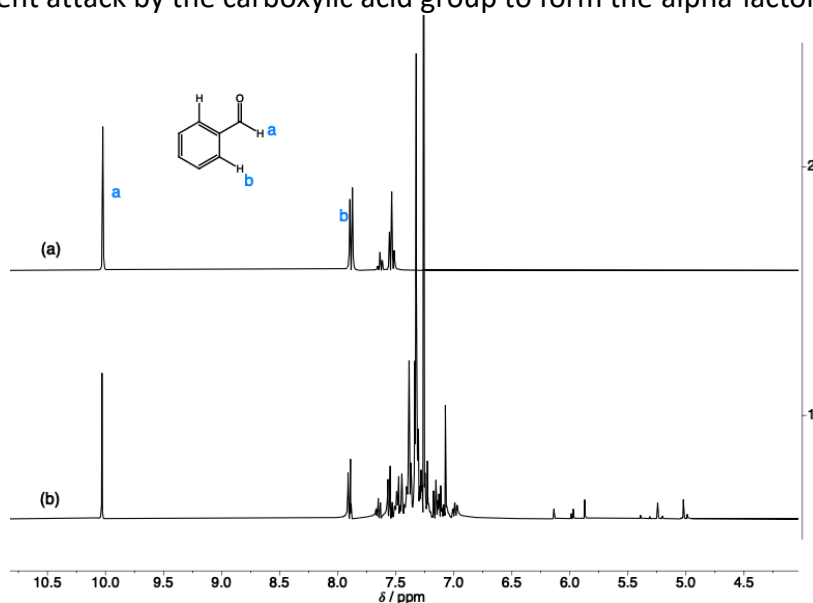


Figure S9  $^1\text{H}$  NMR spectra (400 MHz,  $\text{CDCl}_3$ ) of: (a) benzaldehyde, (b) product mixture from H-Beta-75-catalysed reaction of mandelic acid. Reaction conditions: 2g mandelic acid, 1.3 g zeolite H-Beta-75, 20 mL mixed xylenes, reflux with Dean Stark trap, Oil bath  $T = 175^\circ\text{C}$  ( $T_b + 35^\circ\text{C}$ ), stirring rate = 500 rpm, time = 2 hours.

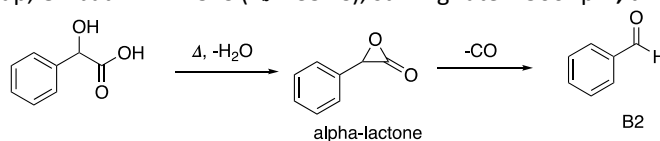


Figure S10 Gas phase decomposition pathway of mandelic acid proposed in the literature.<sup>4</sup>

### 1.4.3 B3. 2,5-diphenyl-1,3-dioxolan-4-one

Dioxolanones are formed from the reaction of an alpha-hydroxy acid and a carbonyl compound. In the case of B3, this occurs from the reaction of mandelic acid and benzaldehyde. In zeolite-catalysed reactions, this product was isolated along with mandelide in the organic layer from aqueous organic extraction of crude product mixtures, and its identification was possible by comparing the  $^1\text{H}$  and  $^{13}\text{C}$  NMR spectra of these zeolite-catalysed products with that of a reference sample synthesised from benzaldehyde and mandelic acid (PTSA used as catalyst, Figure S11).<sup>5</sup> Cis- and trans- isomers of this product are assigned in the literature.<sup>6</sup>

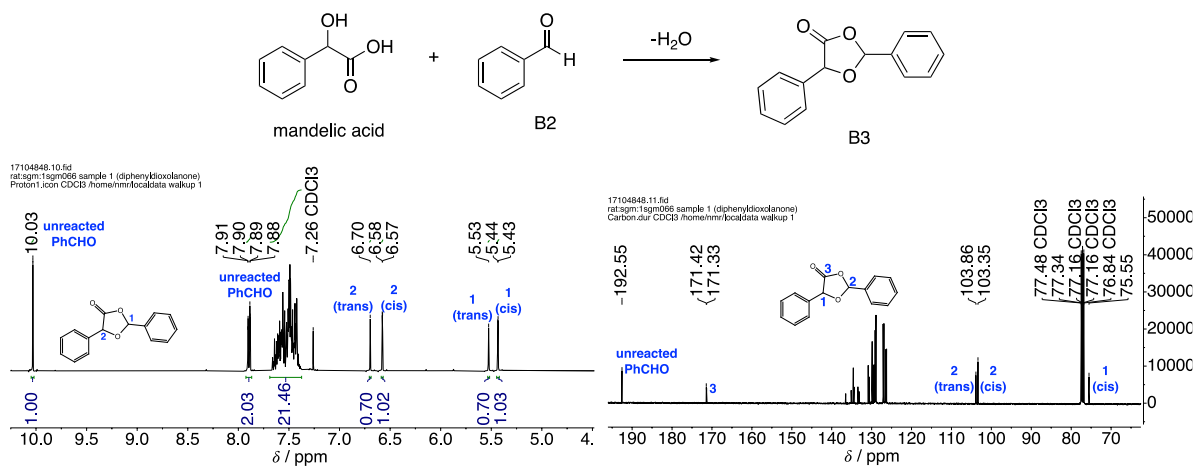


Figure S11 Reaction of mandelic acid with benzaldehyde (B2) to produce byproduct 2,5-diphenyl-1,3-dioxolan-4-one (B3).  $^1\text{H}$  and  $^{13}\text{C}$  NMR spectra in  $\text{CDCl}_3$  (400 MHz) of dioxolanone synthesised by reaction of mandelic acid and benzaldehyde in methylcyclohexane according to a literature procedure.<sup>5</sup> Conditions: reflux with Dean Stark trap overnight. 1 g mandelic acid, 0.68 mL benzaldehyde (1 eqv.), 10 ml methylcyclohexane. Yield approximately 56 %.

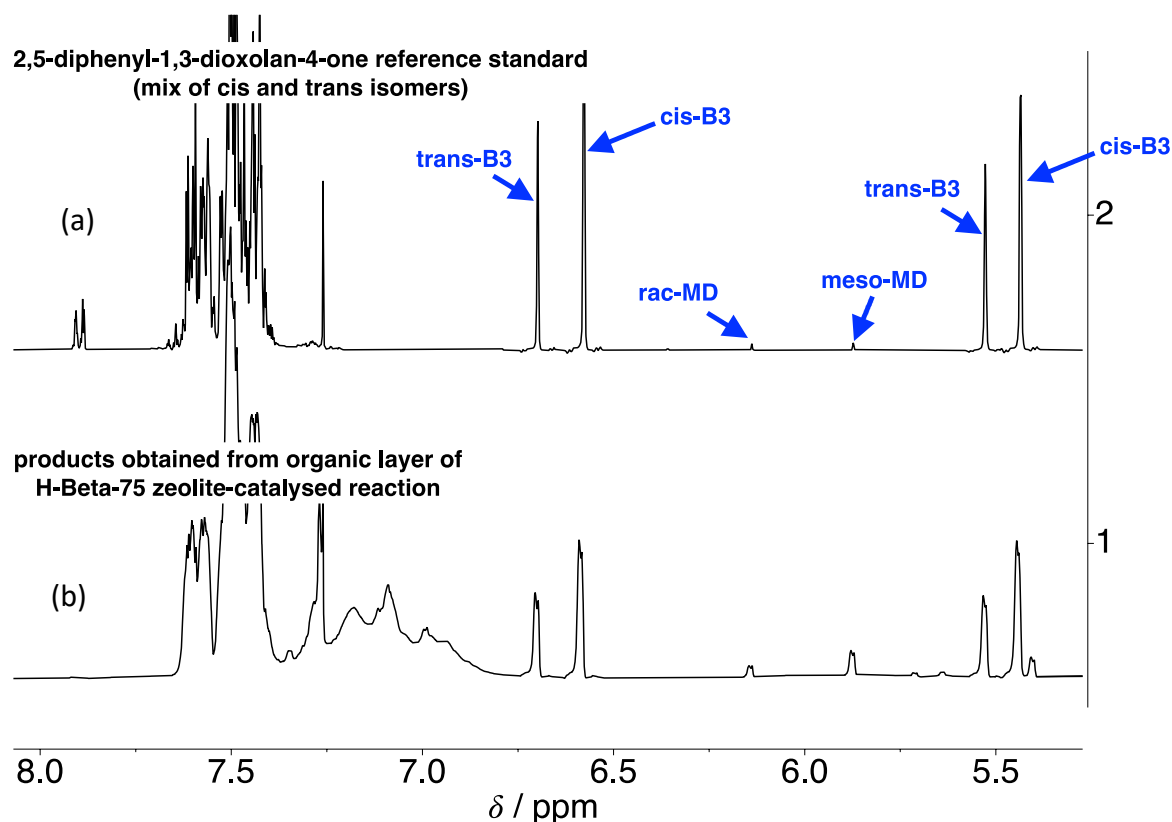


Figure S12  $^1\text{H}$  NMR spectra (400 MHz,  $\text{CDCl}_3$ ). (a) 2,5-diphenyl-1,3-dioxolan-4-one (B3) reference compound synthesised via literature procedure; (b) products obtained from the organic layer after organic/aqueous extraction of a H-Beta-75 zeolite-catalysed product mixture.

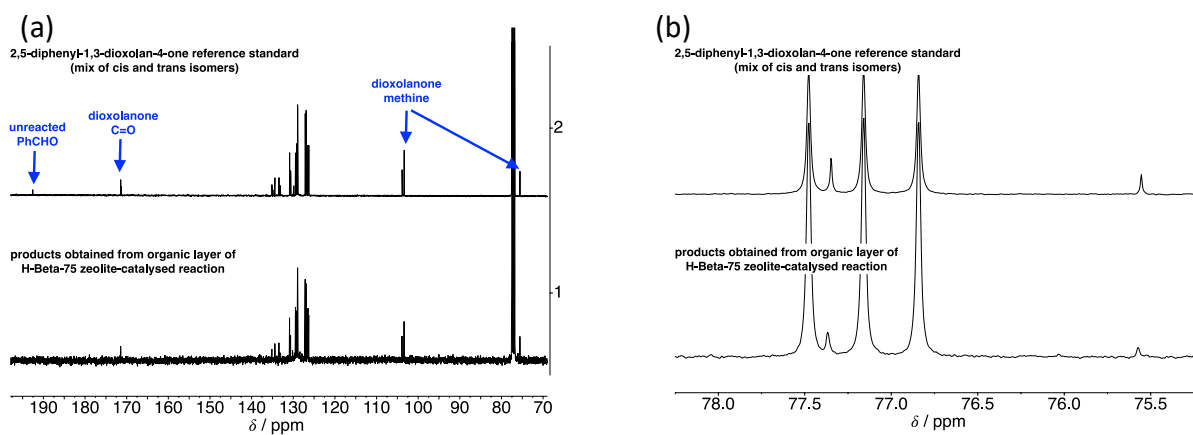


Figure S13  $^{13}\text{C}$  NMR spectra (400 MHz,  $\text{CDCl}_3$ ). (a) TOP: 2,5-diphenyl-1,3-dioxolan-4-one (B3) reference compound synthesised via literature procedure; BOTTOM: products obtained from org/aq extraction of a zeolite-catalysed product mixture. Reference standard contains some unreacted benzaldehyde (carbonyl peak annotated). (b) the same stacked spectra expanded around the residual solvent peak to show the methine peaks of the *cis* (77.3 ppm) and *trans* isomers (75.6 ppm).

#### 1.4.4 Quantification Method and an Example Product Mixture Quantification

The method of quantification employed was based on the <sup>1</sup>H NMR method reported by Sels et al.<sup>7</sup> Quantification was conducted for the following compounds and their structural isomers: mandelic acid, mandelide linear dimer, cyclic mandelide, electrophilic aromatic substitution (B1), benzaldehyde (B2) and diphenyldioxolanone (B3) – shown in Figure S2. The amount of each compound was quantified in terms of the amount of mandelic acid incorporated into the products by integrating the methine resonances of mandelic acid, mandelide linear dimer, cyclic mandelide, electrophilic aromatic substitution (B1) and diphenyldioxolanone (B3). In the case of benzaldehyde (B2), the aldehyde peak was used. The quantity of each compound is then calculated by:

$$\text{compound A (\%)} = \frac{\text{sum of methine integrals for compound A}}{\text{sum of methine and aldehyde integrals}} \times 100\%$$

From this, conversion and selectivity can be defined as:

$$\text{conversion (\%)} = 100\% - \text{mandelic acid (\%)}$$

$$\text{selectivity compound A (\%)} = 100\% \times \frac{\text{compound A (\%)}}{\text{conversion (\%)}}$$

Each reaction was repeated multiple times (at least twice). The reproducibility of catalytic tests was evaluated by 3-fold repetition of a test run with the following reaction conditions: mandelic acid (0.2 g), 3 mol% Al (H-Beta-75), mixed xylenes (20 ml), 1 hour reaction time. The deviation of the arithmetic mean of obtained conversion and selectivity results was below 3%, as shown in Table S1 below.

Table S1 Individual conversion and selectivity data used to determine the standard deviation of catalytic tests. All values given as %.

	<b>Conversion</b>	<b>Linear dimer</b>	<b>Mandelide</b>	<b>B1</b>	<b>B3</b>	<b>B2</b>
<b>Run 1</b>	45	21	24	27	10	15
<b>Run 2</b>	44	20	21	28	9	19
<b>Run 3</b>	48	24	24	26	8	17
<b>Mean</b>	<b>45</b>	<b>21</b>	<b>23</b>	<b>27</b>	<b>9</b>	<b>17</b>
<b>Standard deviation</b>	<b>2</b>	<b>2</b>	<b>2</b>	<b>1</b>	<b>1</b>	<b>2</b>

The method of quantification is illustrated below using the reaction of mandelic acid with toluene, catalysed by H-Beta-75 as this reaction results in the widest product distribution. The reaction produces both diastereomers of mandelide, rac mandelide (r-MD) and meso-mandelide (m-MD), as well as all three of the key products, B1-B3. Key regions of the proton NMR spectrum used to quantify each compound are shown in Figure S14.

The integrals shown annotated on the spectra have been normalised such that the sum of all the methine protons is 1, and displayed to 2 d.p. for clarity. Absolute integral values were used for all calculations. A summary of the methine integrals, along with assignments and the final product distributions, is shown Table S1. In the case of toluene, the methine shift of one of the positional isomers of the B1 product overlaps with the mandelic acid peak. By comparing the methyl CH<sub>3</sub> peaks of the B1 products (Figure S14c) to the total sum of the methine peaks, it is possible to calculate the content of the B1 product as around 43%, slightly higher than the 38% calculated from the two peaks at 5.24 and 5.02. Whilst this suggests a slight inaccuracy of the method due to overlapping peaks, the 5% difference is small and not dissimilar to the expected variation that will arise from this method of NMR spectroscopic quantification.

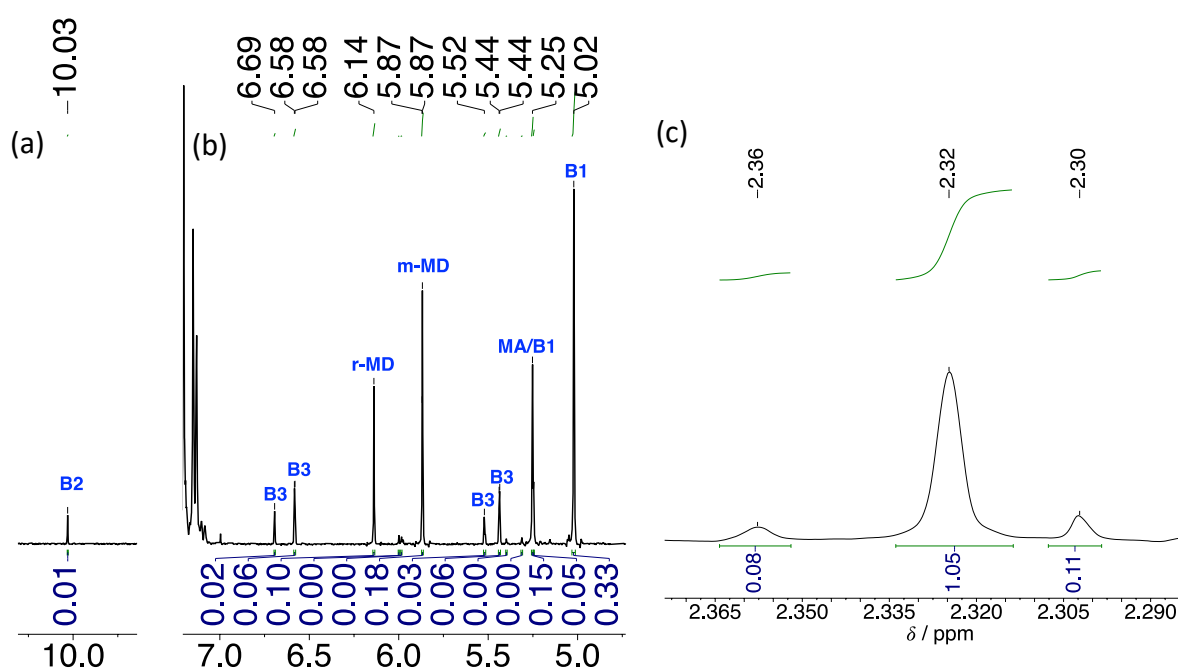


Figure S14 Key regions of the <sup>1</sup>H NMR spectrum (400MHz, CDCl<sub>3</sub>) of products obtained from reaction of mandelic acid in the presence of H-Beta-75 catalyst, carried out in refluxing toluene with azeotropic water removal. (a) benzaldehyde peak at around 10 ppm, (b) methine region containing the methine proton peaks, (c) methyl CH<sub>3</sub> protons of byproduct B1 corresponding to the three possible isomers.

Table S2 Integrals from the <sup>1</sup>H NMR spectrum shown in Figure S14.

Integral Range / ppm	Integral / %	assignment
10.03 - 10.03	1	PhCHO (B2)
6.70 - 6.69	2	diphenyldioxolanone (B3)
6.59 - 6.58	6	
6.14 - 6.13	10	rac-mandelide (r-MD)
6.00 - 6.00	0	Mandelic acid dimers
5.99 - 5.98	0	
5.87 - 5.86	18	meso-mandelide (m-MD)
5.53 - 5.51	3	diphenyldioxolanone (B3)
5.44 - 5.43	6	
5.40 - 5.39	0	Mandelic acid dimers
5.32 - 5.31	0	
5.26 - 5.25	14	mandelic acid/meta-B1 (signal overlap)
5.25 - 5.24	5	ortho-B1
5.03 - 5.01	33	para-B1

Table S3 Product quantification based on integrals in 2. The total for each compound is calculated by the sum of the integration of its methine proton peaks, which equates to the amount of mandelic acid consumed to make each product. In the case of product B1, the peak corresponding to meta isomer overlaps with the residual mandelic acid peak when NMR is recorded in CDCl<sub>3</sub>. As a result, quantification by the methine protons gives an underestimation of B1 compared with using the peaks for Ar-CH<sub>3</sub> protons that occur separately at around 2.3 ppm.

Compound	distribution / %
Mandelic acid	14 (around 9% if effect of meta-B1 overlap accounted for)
Mandelide	27
B1 (using methine <b>CH</b> ) <sup>a</sup>	38
B1 (using methyl Ar- <b>CH<sub>3</sub></b> ) <sup>b</sup>	43
B2	1
B3	17

<sup>a</sup> : distribution (%) = 100 x (B1 methine **CH** integral)/sum of all compound methine CH integrals

<sup>b</sup> : distribution (%) = 100 x (B1 Ar-**CH<sub>3</sub>** integral/3)/sum of all methine CH integrals



## 2 Effect of Reaction Conditions on Product Distribution in Mandelic Acid Conversion using H-Beta-75 and H-USY Zeolites as Catalyst

### 2.1 Effect of Reaction Solvent on Selectivity with H-Y-30 Catalyst

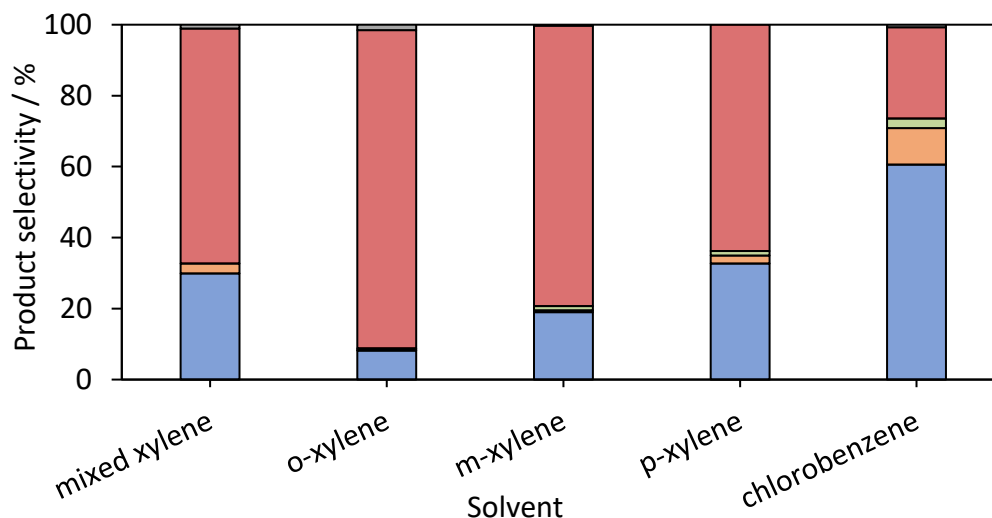


Figure S15 Selectivity and conversion to arylation products catalysed by H-Y-30 zeolite. Conditions: 0.5 g mandelic acid in 50 ml solvent, 3.5 mol% H-Y-30 catalyst, reflux with Dean Stark trap. Stirring rate = 500 rpm. Reactions were run for 1 hour under reflux at the boiling point of each solvent. Product distributions calculated based on integration of  $^1\text{H}$  NMR spectra recorded at 400 MHz in  $\text{CDCl}_3$ . Aside from p-xylene and mesitylene, products are obtained as a mixture of positional isomers, with the para isomer the major product.

### 2.2 Effect of Reaction Solvent on H-Beta-75 Catalysis

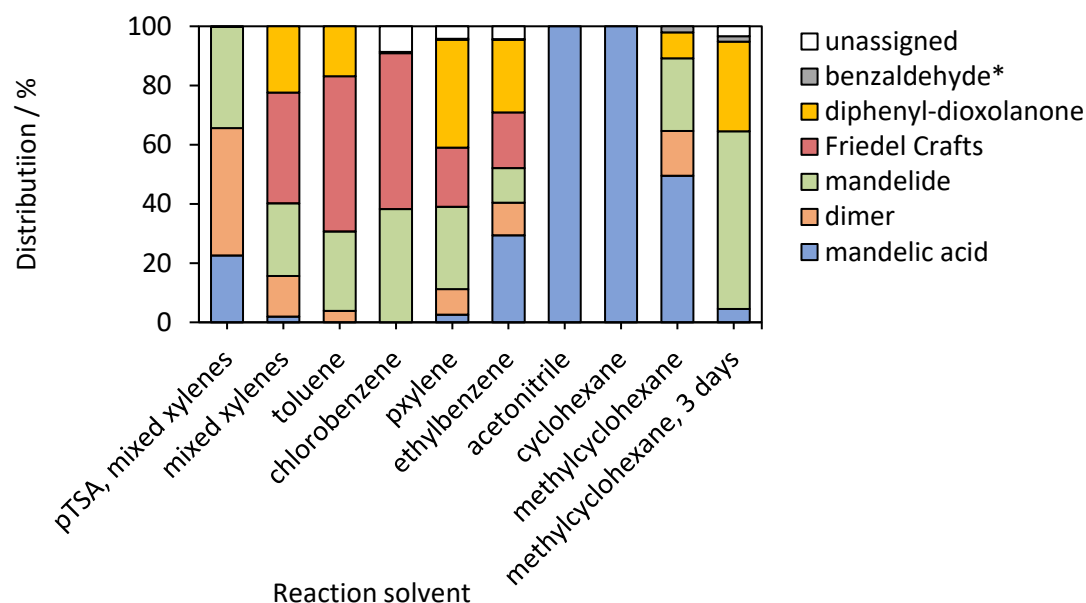


Figure S16 Product distributions from catalyst screening. Conditions: 0.5 g mandelic acid in 50 ml solvent, 3.5 mol% H-Beta-75 catalyst, reflux with Dean Stark trap overnight (ca. 20 hours) with the exception of the second 3-day reaction in methylcyclohexane, stirring rate = 500 rpm. Product distributions calculated based on integration of  $^1\text{H}$  NMR spectra recorded at 400 MHz in  $\text{CDCl}_3$ .

### 2.3 Selectivity of Commercial Zeolites H-Beta-75, H-Y-30, H-MOR-97 and H-ZSM-45 at Low and Near Iso-conversion of Mandelic Acid

Due to the effect of sequential catalyst reactions, catalyst product selectivity is best compared at very similar conversion levels.<sup>8,9</sup> Hence a study of zeolites H-Beta-75, H-Y-30, H-MOR-97 and H-ZSM-45 at 25-30 % conversion was undertaken in order to evaluate catalyst/product selectivity.

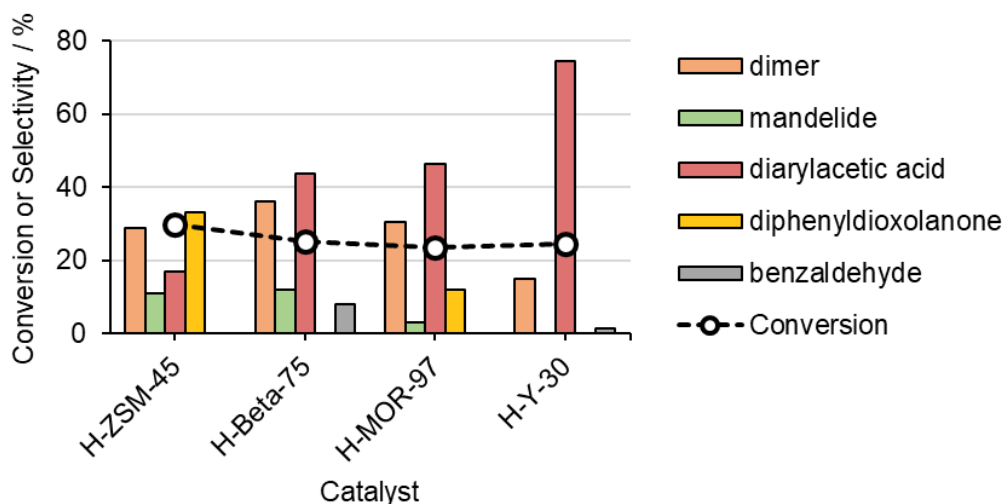


Figure S17 Product distribution and conversion for reaction of mandelic acid showing the variation in selectivity at near iso-conversion. Reaction conditions: 0.2 g mandelic acid in 20 ml mixed xylenes, reflux with Dean Stark trap for various reaction times (H-Beta-75: 40 minutes, H-USY-30: 5 minutes, H-ZSM5-45: 20 hours), stirring rate = 500 rpm. Product distributions calculated based on integration of <sup>1</sup>H NMR spectra recorded at 400 MHz in CDCl<sub>3</sub>

Figure S17 shows selectivity of H-MOR-97, H-Beta-75, H-USY-30 and H-ZSM5-45 at 24, 25, 25 and 30 % conversion, respectively. H-Beta-75 and H-ZSM5-45 appear to give similar selectivity for dimerization of mandelic acid to mandelide, with a combined selectivity towards dimer and mandelide of around 48 % and 40 %, respectively. H-USY-30 catalyses the electrophilic aromatic substitution reaction (Friedel-Crafts product, B1) at 76 % selectivity.

### 3 Molecular Size and Zeolite Pore Considerations

Approximations of the size of some of the key molecules were modelled using an approach that has been successfully reported recently.<sup>10, 11</sup> Molecular sizes were approximated by first carrying out an energy minimisation at the B3LYP level using Scigress<sup>12</sup> then transferred into the VMD visualisation program.<sup>13</sup> The energy minimised molecules were rotated to find and calculate the minimum projection area using the separation between the two furthest atoms (from van der Waal's radii). The values of these minimum cross section diameters are given in Tables S4.

Beta catalysts form a mix of products which may be attributed to catalysis occurring on the external surface of the zeolite and the absence of any shape selectivity effects. H-Y-30 shows selectivity for the electrophilic aromatic substitution reaction, producing diarylacetic acids selectively. The selectivity may be attributed to reactions occurring in the pores of zeolite Y between mandelic acid and solvent molecules, as both should fit within the pores. However, the size calculations indicate that the diarylacetic acid product of p-xylene and mandelic acid (the largest of all observed products at 8.4 Å) should not be able to leave the super cage (sphere of inclusion = 11.2 Å) by diffusing through the zeolite Y pore window (7.4 Å). Therefore the selectivity observed with hierarchical zeolite H-Y-30 may arise from more accessible (partial) super cages, possibly at the surface of the crystal.

Table S4 Molecular cross section calculated for key molecules in conversion of mandelic acid by zeolites.

Molecule	Radius / Å
mandelic acid	7.1
mandelide	7.3
diphenyldioxolanone	7.4
Diarylacetic acid (p-xylene)	8.4

Table S5 Zeolite framework properties taken from the IZC database.<sup>14</sup>

Framework	Channel system	Channels / Å	Max sphere included / Å	Max sphere diffuse / Å
ZSM5	3D	10 MR: 5.2 x 5.7 5.3 x 5.6	6.36	4.7, 4.46
Beta	3D	12MR: 6.6 x 6.6 5.6 x 5.6	6.68	5.95
Y (FAU)	3D	12 MR: 7.4 x 7.4	11.24	7.35

## 4 Zeolite Catalyst Properties

Table S6 Si/Al ratios of commercial zeolites.

Zeolite	Supplier/Code	Nominal Si/Al	Mass of zeolite (g) used at 3 mol% Al <sup>(a)</sup>	Si/Al <sup>(b)</sup>
H-Beta-12.5	Clariant/CZB25	12.5	0.032	18.1
H-Beta-15	Clariant/CZB30	15.0	0.038	16.5
H-Beta-75	Clariant/CZB150	75	0.18	53.0
H-ZSM5-15	Clariant/CZP30	15	0.038	
H-ZSM5-45	Clariant/CZP90	45	0.11	40.6
H-Y-2.5	JM/CBV400	2.55	0.0090	3.0
H-Y-15	JM/CBV720	15	0.038	15.0
H-Y-30	Alfa Aesar/CBV760	30	0.074	26.5
H-Y-40	Alfa Aesar/CBV780	40	0.098	46.1
H-L-3	Clariant/CZL6	3	0.0096	2.9
H-MOR-10	Clariant/CZM20	10	0.026	

<sup>(a)</sup> Mass of zeolite used for time dependent conversion studies: 0.2 g mandelic acid, 3 mol% Al, 20 ml solvent, 50 ml round bottom flask.

<sup>(b)</sup> Determined by EDXRF

The CBV series of high silica zeolite Y (currently produced by Zeolyst, previously known as PQ Corporation / Shell) is made by a sequence of steps which involve steaming and acid washing, forming hierarchical materials with well-established micro- and mesoporosity.<sup>15-17</sup> Reported textural properties of CBV catalysts used in this study are given in Table S7, along with those of the CZB (Clariant, Beta zeolite) series. For both the CBV and CZB series, higher Si/Al ratios give rise to lower fractions of micropore volume, indicative of increasing mesoporosity and hierarchical structures. It has been noted that the number of external acid sites on zeolite H-Y-30 (CBV760) represents only 4 % of its total acid sites,<sup>18</sup> despite the mesoporous nature of the material.

Table S7 Reported textural properties of commercial H-Beta and H-Y catalysts.

Zeolite	$V_{\text{total}} / \text{cm}^3 \text{g}^{-1}$	$V_{\text{micro}} / \text{cm}^3 \text{g}^{-1}$	BET Surface Area / $\text{m}^2 \text{g}^{-1}$	$S_{\text{meso}} / \text{m}^2 \text{g}^{-1}$	$S_{\text{ext}} / \text{m}^2 \text{g}^{-1}$	Ref
H-Beta-15 (CZB30)	0.36	0.22	546	118		19
H-Beta-75 (CZB150)	0.49	0.20	516	126		19
H-Y-2.5 (CBV400)	0.30	0.26	721		72	20
H-Y-15 (CBV720)	0.54	0.32	760	144		21
H-Y-30 (CBV760)	0.56	0.32	797	171		21
	0.54	0.27	805		261	18
	0.53	0.34	913		313	22
H-Y-40 (CBV780)	0.52	0.26	734	226		21
	0.528	0.277				15

Table S8 Reported acidity properties of commercial H-Beta and H-Y catalysts.

Zeolite	Brønsted <sup>a</sup> / $\mu\text{mol g}^{-1}$	Lewis <sup>a</sup> / $\mu\text{mol g}^{-1}$	B/L <sup>b</sup>	Ref
H-Beta-15 (CZB30)	150	85	1.8	19
H-Beta-75 (CZB150)	66	8	8.3	19
H-Y-2.5 (CBV400)	230	180	1.3	20
H-Y-2.5 (CBV300)	584	207	2.8	21
H-Y-15 (CBV720)	220	69	3.2	21
H-Y-30 (CBV760)	151	37	4.1	21
	240	84	2.9	18
H-Y-40 (CBV780)	52	8	6.5	21

<sup>a</sup>Concentrations of Brønsted and Lewis acid sites derived from pyridine-IR

<sup>b</sup> Ratio of Brønsted and Lewis acid sites

## 4.1 Comparison of HY series

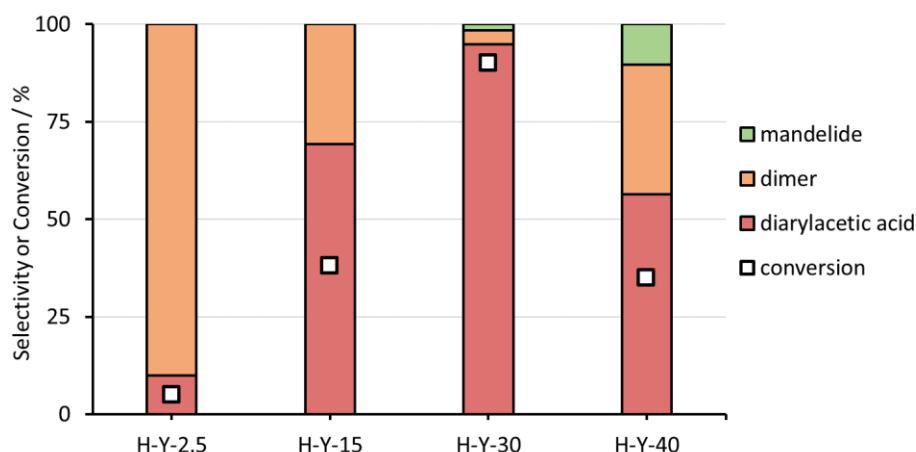


Figure S18 Product distribution and conversion for reaction of mandelic acid showing the variation in selectivity for the HY series. Reaction conditions: 0.2 g mandelic acid in 20 ml mixed p-xylene, reflux with Dean Stark trap for 1 hour reaction time, stirring rate = 500 rpm. Product distributions calculated based on integration of  $^1\text{H}$  NMR spectra recorded at 400 MHz in  $\text{CDCl}_3$

Testing of the Zeolyst CBV series of H-Y materials (H-Y-2.5, H-Y-15, H-Y-30 and H-Y-40) shows that the FAU framework avoids the formation of benzaldehyde and 2,5-diphenyl-1,3-dioxolan-4-one (DOX) unlike the Beta series (Figure 1), highlighting that the framework governs the product distribution. This is despite the variations in textural properties (micropore and mesopore) and Si/Al ratio.

Notably, H-Y-40 gave lower mandelic acid conversion and selectivity to the diarylacetic acid product than H-Y-30, but without the formation of benzaldehyde and 2,5-diphenyl-1,3-dioxolan-4-one (DOX). Textural and acidic properties reported by Perez-Ramirez *et al.*<sup>21</sup> show HY40 to have a lower Lewis acid site concentration ( $B/L = 6.5$ ) compared to HY30 ( $B/L = 4.1$ ), while HY40 has increased mesoporosity.

## 4.2 Estimate of occluded organic matter in H-Y-30 post reaction

The extent of organic matter occluded in the H-Y-30 catalyst post reaction was estimated by evaluating the mol % of unaccounted for organic matter. For one of the experiments shown in Figure 2 (0.2 g mandelic acid, 0.074 g H-Y-30, 20 ml mixed xylenes, time = 1 hour, 91% conversion), only a mix of unreacted mandelic acid and diarylacetic acids was detected by NMR. The crude mass of organic matter recovered after reaction workup (rotary evaporation) was measured. Based on the level of conversion and resultant relative molecular mass (RMM), 17 mol% of the organic matter is missing from the final isolated reaction mixture. Assuming all of this is occluded on the zeolite (worst case scenario, as some losses are likely caused from the experimental workup) then 17% of the organic matter is occluded on the zeolite. The calculation is shown in the table below:

Mandelic acid at start / g	0.1999
Crude product mass / g	0.2522
Conversion (from <sup>1</sup> H NMR) / %	91
Mandelic acid RMM / gmol <sup>-1</sup>	152.15
Diarylacetic acid RMM / gmol <sup>-1</sup>	240.3
<b>Mandelic acid at start / mmol</b>	<b>1.31</b>
RMM of crude product mixture / gmol <sup>-1</sup> (91 % Diarylacetic acid & 9 % Mandelic acid)	232.37
<b>Crude product mixture / mmol</b>	<b>1.09</b>
Theoretical occluded / mmol	0.23
<b>Theoretical occluded / %</b>	<b>17</b>

TGA analysis was also conducted on this sample and shows a 7% weight loss between 140 °C and 800 °C (Perkin Elmer TGA 8000, 50 mL min<sup>-1</sup> dry air, room temperature to 800 °C, ramp 10 °C/min<sup>-1</sup>, held isothermally at 140 °C for 1 h to remove solvents). This in line with the occluded organic material calculation, and shows that only small amounts of organic matter (approximately 10 mol%) are likely trapped/ or missing from selectivity calculations.

### 4.3 A comment on catalyst lifetime

In order to evaluate whether the H-Y-30 catalyst is still active after conversion of the initial charge of mandelic acid, additional charges were added. Under the following reaction conditions (0.2 g mandelic acid, 0.074 g H-Y-30, 20 ml p xylene, 1 hour reflux), two additional portions of mandelic acid were added after one hour intervals directly to the reaction flask. A modest increase in diarylacetic acid formation occurred after addition of the second reagent charge, but not after the third. The results are shown below:

Reaction time elapsed / h	Cummulative amount of Mandelic acid added / mmol	Mole fraction of Diarylacetic acid (by <sup>1</sup> H NMR)	Cummulative amount of Diarylacetic acid produced / mmol
1	1.35	0.888	1.20
2	2.73	0.505	1.38
3	4.05	0.343	1.39

This result indicates that catalyst activity is attenuated after the 1<sup>st</sup> reaction. It is unclear at whether this is caused by product inhibition of the catalyst. An intermediate calcination step to reactivate the catalyst was not undertaken but may be required to reactivate the catalyst.

## References

1. J. K. Whitesell and J. A. Pojman, *Chem. Mater.*, 1990, **2**, 248-254. "Homochiral and heterochiral polyesters: polymers derived from mandelic acid".
2. T. Q. Liu, T. L. Simmons, D. A. Bohnsack, M. E. Mackay, M. R. Smith and G. L. Baker, *Macromolecules*, 2007, **40**, 6040-6047. "Synthesis of polymandelide: A degradable polylactide derivative with polystyrene-like properties".
3. G. J. Graulus, N. Van Herck, K. Van Hecke, G. Van Driessche, B. Devreese, H. Thienpont, H. Ottevaere, S. Van Vlierberghe and P. Dubruel, *React. Funct. Polym.*, 2018, **128**, 16-23. "Ring opening copolymerisation of lactide and mandelide for the development of environmentally degradable polyesters with controllable glass transition temperatures".
4. I. M. Gabriel Chuchani, *J. Phys. Org. Chem.*, 1997, **10**, 121-124. "Elimination Kinetics of DL-Mandelic Acid in the Gas Phase".
5. S.-S. Weng, H.-C. Li and T.-M. Yang, *RSC Adv.*, 2013, **3**, 1976-1986. "Chemoselective esterification of  $\alpha$ -hydroxyacids catalyzed by salicylaldehyde through induced intramolecularity".
6. V. A. Shcherbinin and V. V. Konshin, *Tetrahedron*, 2019, **75**, 3570-3578. "Convenient synthesis of O-functionalized mandelic acids via Lewis acid mediated transformation of 1,3-dioxolan-4-ones".
7. M. Dusselier, P. Van Wouwe, A. Dewaele, P. A. Jacobs and B. F. Sels, *Science*, 2015, **349**, 78-80. "Shape-selective zeolite catalysis for bioplastics production".
8. T. Bligaard, R. M. Bullock, C. T. Campbell, J. G. Chen, B. C. Gates, R. J. Gorte, C. W. Jones, W. D. Jones, J. R. Kitchin and S. L. Scott, *ACS Catal.*, 2016, **6**, 2590-2602. "Toward Benchmarking in Catalysis Science: Best Practices, Challenges, and Opportunities".
9. F. Schüth, M. D. Ward and J. M. Buriak, *Chem. Mater.*, 2018, **30**, 3599-3600. "Common Pitfalls of Catalysis Manuscripts Submitted to Chemistry of Materials".
10. T. C. Keller, S. Isabetini, D. Verboekend, E. G. Rodrigues and J. Pérez-Ramírez, *Chem. Sci.*, 2014, **5**, 677-684. "Hierarchical high-silica zeolites as superior base catalysts".
11. F. C. Hendriks, D. Valencia, P. C. A. Bruijninx and B. M. Weckhuysen, *Phys. Chem. Chem. Phys.*, 2017, **19**, 1857-1867. "Zeolite molecular accessibility and host-guest interactions studied by adsorption of organic probes of tunable size".
12. Fujitsu: Integrated Platform for Computational Chemistry SCIGRESS., <https://www.fujitsu.com/global/solutions/business-technology/tc/sol/scigress/>, (accessed 23rd March 2023).
13. W. Humphrey, A. Dalke and K. Schulten, *J. Molec. Graphics*, 1996, **14**, 33-38. "VMD - Visual Molecular Dynamics".
14. C. Baerlocher and L. McCusker, Database of Zeolite Structures, <http://www.iza-structure.org/databases/>, (accessed 23rd March 2023).
15. A. H. Janssen, A. J. Koster and K. P. de Jong, *Angew. Chem. Int. Ed.*, 2001, **40**, 1102-1104. "Three-Dimensional Transmission Electron Microscopic Observations of Mesopores in Dealuminated Zeolite Y".
16. K. P. de Jong, J. Zečević, H. Friedrich, P. E. de Jongh, M. Bulut, S. van Donk, R. Kenmogne, A. Finiels, V. Hulea and F. Fajula, *Angew. Chem. Int. Ed.*, 2010, **49**, 10074-10078. "Zeolite Y Crystals with Trimodal Porosity as Ideal Hydrocracking Catalysts".
17. J. Kenvin, S. Mitchell, M. Sterling, R. Warringham, T. C. Keller, P. Crivelli, J. Jagiello and J. Perez-Ramirez, *Adv. Funct. Mater.*, 2016, **26**, 5621-5630. "Quantifying the Complex Pore Architecture of Hierarchical Faujasite Zeolites and the Impact on Diffusion".



18. L. Lakiss, A. Vicente, J. P. Gilson, V. Valtchev, S. Mintova, A. Vimont, R. Bedard, S. Abdo and J. Bricker, *ChemPhysChem*, 2020, **21**, 1873-1881. "Probing the Bronsted Acidity of the External Surface of Faujasite-Type Zeolites".
19. R. Lin, S. Mitchell, T. Netscher, J. Medlock, R. T. Stemmler, W. Bonrath, U. Létinois and J. Pérez-Ramírez, *Catal. Sci. Tech.*, 2020, **10**, 4282-4292. "Substrate substitution effects in the Fries rearrangement of aryl esters over zeolite catalysts".
20. Y. Chapellière, C. Daniel, A. Tuel, D. Farrusseng and Y. Schuurman, *Catalysts*, 2021, **11**, 652. "Kinetics of n-Hexane Cracking over Mesoporous HY Zeolites Based on Catalyst Descriptors".
21. T. C. Keller, J. Arras, S. Wershofen and J. Pérez-Ramírez, *ACS Catal.*, 2015, **5**, 734-743. "Design of Hierarchical Zeolite Catalysts for the Manufacture of Polyurethane Intermediates".